



Kinetic, isotherm and pH dependency investigation and environmental application of cationic dye adsorption on montmorillonite

Ayşe Erçağ^a, Pelin Demirçivi^b, Jülide Hızal^{b,*}

^aFaculty of Engineering, Department of Chemistry, İstanbul University, İstanbul 34320, Turkey, Tel. +90 2124717703; Fax: +90 2124737180; email: ercağa@istanbul.edu.tr (A. Erçağ)

^bFaculty of Engineering, Department of Chemical and Process Engineering, Yalova University, Yalova 77100, Turkey, Tel. +90 2268155391; Fax: +90 22681126551; emails: pdemircivi@yalova.edu.tr (P. Demirçivi), hizalyucesoy@yalova.edu.tr (J. Hızal)

Received 20 March 2014; Accepted 26 August 2014

ABSTRACT

In this study, individual and competitive adsorption of three cationic dye onto montmorillonite were investigated. Langmuir, Freundlich, Temkin, and Dubinin–Radushkevich isotherm models were used to analyze experimental data for individual and competitive adsorption of dyes. Surface precipitation occurred in the presence of inert electrolyte because of decreasing solubility of dye. The organic dye adsorption was pH-independent in a pH scale between 2 and 6. It is, thus, assumed that the adsorption took place between cationic organic dye and permanently negatively charged surface, which is a pH-independent surface site of adsorbent and occurred as a result of isomorphic substitution. Mean free energies (E_D) varied between 0.65 and 7.87 J/mol, and heats of sorptions (B) changed between 4 and 96 J/mol. These low energy values support the electrostatic interaction between surface and dye molecules. Organic dye adsorption showed Langmuirian character and in the presence of more than one adsorptive dye, adsorption capacities remained under individual adsorption capacity values because of competition. Adsorption kinetic showed second order reaction character. Using sodium humate, CaCl₂ solution, and acid mixture solution as leach solutions desorption properties were examined. Higher desorption values were achieved by using 1% of sodium humate solution because of hydrophobic interactions and formation of H bonds.

Keywords: Kinetic; Adsorption; Desorption; Competitive adsorption; Intraparticle diffusion

1. Introduction

Water pollution is a significant environmental problem that threaten our future. Water treatment of textile industrial waste waters is respectively difficult than that of other industrial waste waters because of their chemical ingredients such as organic dyes. After

discharging of textile waste water, organic dyes form a colored layer on the water surface, preventing sunlight entrance into deeper layers, inhibiting submarine photosynthetic reactions. Also, organic dye molecules cause formation of toxic and carcinogenic waste products in aquatic media. So, removal of organic dyes from watercourse and marine environment has vital importance. It is difficult to remove these organic dyes

*Corresponding author.

using conventional oxidation and biodegradation method, because the azo groups are stable against oxidizing agent, temperature, and UV light.

Many separation methods, such as flocculation-coagulation, reverse osmosis and adsorption, have been used for removal of organic dyes from textile industrial waters. As a low cost and feasible process, adsorption is preferred amongst other methods [1]. It is an effective method and gives better results for removing different types of coloring materials from waste water [2]. Activated carbon, chitosan, lignin, fly ash, and clays are commonly used adsorbents in various studies. Carbon nanotubes and many organic resin such as cyclodextrin are also used as adsorbent. Kuo et al. tried direct dye adsorbent on carbon nanotubes in terms of isotherm, thermodynamic, and kinetic properties using different kinetic models, and mentioned that direct dye adsorption on carbon nanotube fits Freundlich isotherm and pseudo-second order reaction kinetic. And also, intraparticle diffusion contributes to mass transfer of dye [3]. On the other hand, clay minerals have been widely used for the purpose of water treatment, because of their abundance and high affinity for both hydrophobic and hydrophilic pollutants. All studies about dye removal with clay minerals showed that basic organic dye adsorption on clays increased with increasing pH and initial concentration of dye, and contact time changed between 30 min and 2 h [4–11]. Fil et al. investigated Basic Red 18, Basic Violet 16, and Methyl Violet Dye adsorption on montmorillonite as a function of contact time, initial dye concentration, pH, and temperature, and explained that pseudo-second order kinetic model provided good correlation for the adsorption. They also searched the thermodynamic parameters of dye adsorption on montmorillonite and mentioned that adsorption of these cationic dyes on montmorillonite is endothermic reaction and gibbs free energy of this reaction is greater than zero which shows the un-spontaneous nature of the adsorption model [12–14]. The authors explained that the positive ΔS° values of methyl violet adsorption increase randomness [14].

In this study, individual and competitive adsorption of basic organic dyes which are commercially named as Red 46, Blue 41, and Basic Yellow 28 onto montmorillonite were searched in terms of isotherm, pH effect, and kinetic properties. Furthermore, the desorption properties of these organic dyes into humic acid, acid mixture solution at pH 5, and CaCl_2 solution were investigated. As a result of this study, it is shown that montmorillonite has high adsorption capacity against cationic organic dyes, and thus it is recommended for water treatment of textile industrial water.

2. Materials and methods

2.1. Materials

Basic organic dyes named as Blue 41 ([4-[ethyl (2-hydroxyethyl)amino]phenyl]azo]-6-methoxy-3-methylbenzothiazolium methyl sulfate, 482.57 g/mol), Basic Yellow 28 (2-[[4-methoxyphenyl)methylhydrazono]methyl]-1,3,3-trimethyl-3H-indolium methyl sulfate, 433.52 g/mol), and Red 46 (1H-1,2,4-triazolium, 1,4-dimethyl-5-[[4-[methyl(phenylmethyl)amino]azo]-bromide, 403.32 g/mol) were used in experiments. These dyes were received from AKSA (Akrilik Kimya Sanayi A.Ş.) Company as 100% Red 46 solution ($d_{20} = 1.18$ g/mL), 200% Blue 41 solution ($d_{20} = 1.15$ g/mL), and 100% Basic Yellow 28 solution ($d_{20} = 1.20$ g/mL) in acetic acid. Chemical structures of these dyes are shown in Fig. 1.

Montmorillonite was received from Kalemaden Ceramic Factory at Çanakkale. The chemical analysis of the dry adsorbents yielded the following weight percentages: SiO_2 : 70.45%, Al_2O_3 : 15.80%, TiO_2 : 0.19%, Fe_2O_3 : 1.53%, CaO : 2.02%, MgO : 2.17%, Na_2O : 0.92%, K_2O : 0.57%, and loss on ignition: 6.17%. All chemicals (NaOH , HNO_3 , etc.) used in the experiments were purchased from Merck.

The adsorbent was washed with distilled water until constant pH and dried at 80 °C (Binder ED115). Specific surface area of the adsorbent was measured by B.E.T./ N_2 method (Quantachrome Autosorb 1 MP). Also XRD (PAN Analytical X' Pert Pro) and particle size distribution analysis (Malvern 20 nm–2000 μm Mastersizer 3000) of the adsorbent were performed. Zeta potential of montmorillonite was found as -24.8 mV at pH 6.09 (Zetasizer 3000 HSA).

2.2. Potentiometric titration of adsorbent

Potentiometric titration of montmorillonite sample was performed in a borosilicate reaction vessel in N_2 atmosphere at room temperature. 10 g/L of clay mineral suspension was firstly titrated (ABU 91 Autoburette Radiometer automatic titrator) with 0.1 N HCl and then 0.1 M NaOH solution in the presence of 0.01 M NaClO_4 at a rate of 2 mL/min.

2.3. Batch tests

Kinetic study was performed using Basic Yellow 28 solution of which initial concentration is 3,000 ppm at 25 g/L solid/liquid ratio for 5, 10, 15, 20, 30, 45, 60, 90, and 120 min (Daihan Wise Shake SHO-2D orbital shaker). Twenty milliliter of 3,000 ppm yellow dye solutions were reacted with montmorillonite sample

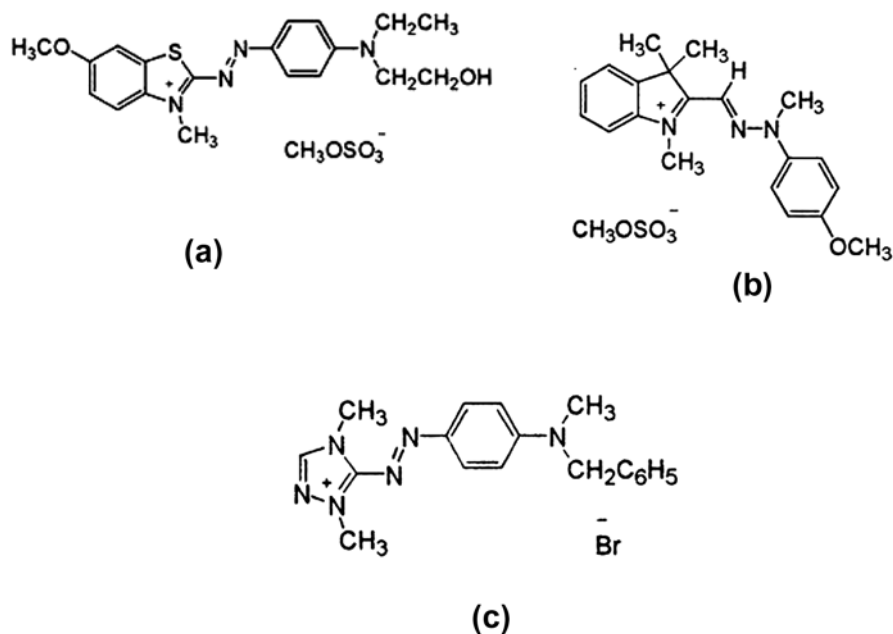


Fig. 1. Chemical structure of basic organic dyes used in experiments (a) Blue 41, (b) Basic Yellow 28, and (c) Red 46.

having 5, 12.5, 20, 25, 30, 33, 37.5, 50, and 75 g/L clay suspension for 30 min at 145 rpm. Isotherm experiments were performed using a batch method at room temperature and constant equilibrium pH (pH 4.5). Initial concentrations of organic dyes changed between 100 and 80,000 ppm. Solid/liquid ratio was maintained at 25 g/L. After 30 min shaking the samples were filtrated, and pH and the absorbance measurements at the related wavelength (λ_{yellow} : 438 nm, λ_{red} : 531 nm, λ_{blue} : 610 nm) were made on the filtrates. The concentration of each dye in mixture filtrate was determined with Derivative Spectroscopic Method using II. Order Derivative absorbance result at each related wavelength (λ_{yellow} : 332 nm, λ_{red} : 554 nm, λ_{blue} : 642 nm). pH dependency of dye adsorption was examined by shaking clay suspension between pH value of 2 and 7. SEM-EDX analysis of loaded adsorbents were performed using (SEM, JEOL Ltd, JSM-5910LV) equipped with EDS (or EDX) (OXFORD Industries INCAx-Sight 7274; 133-eV resolution 5.9 keV) after gold coating.

2.4. Desorption experiments

Desorption experiments were performed using sodium humate solution (at a concentration of 1 and 0.1%), 1 and 0.1 M CaCl_2 solution, and acid mixture (prepared by diluting of 1-to-1 ratio of HCl-HNO_3 mixture until pH 5) solution. The experiments were carried out for 15, 30, 60, 120, 180, 240 min, and also 360 and 480 min for blue/red dye-1% sodium humate /1M

CaCl_2 systems. Absorbance measurements at related wavelength (λ_{yellow} : 438 nm, λ_{red} : 531 nm, λ_{blue} : 610 nm) were made in filtrate after filtration of suspension.

2.5. Adsorption of waste water sample on montmorillonite

For testing the treatability of textile industrial waste water adsorption onto montmorillonite, 20 mL of waste water sample (studied in 24 h after discharge), received from dyeing unit of AKSA Company, was dispersed with 0.5 g montmorillonite at room temperature for 30 min. Following the filtration, chemical oxygen demand (COD) value of filtrate was measured. The initial COD value was measured before adsorption.

3. Results and discussion

Specific surface area of montmorillonite was found as $64 \text{ m}^2/\text{g}$. As seen in XRD spectrum (Fig. 2(a)) the adsorbent mainly consists of montmorillonite component. The result of particle size distribution analysis is shown in Fig. 2(b). Fifty percent of the particles have a diameter of $9.24 \mu\text{m}$, and a mean particle diameter is $12.30 \mu\text{m}$. Specific surface area and particle size of many montmorillonite samples vary between 20 and $130 \text{ m}^2/\text{g}$ and $2.5\text{--}250 \mu\text{m}$, respectively [15–19]. So it can be said that because montmorillonite sample used in this study has smaller particle size and higher surface area, it has high adsorption affinity for both organic and inorganic adsorptive materials.

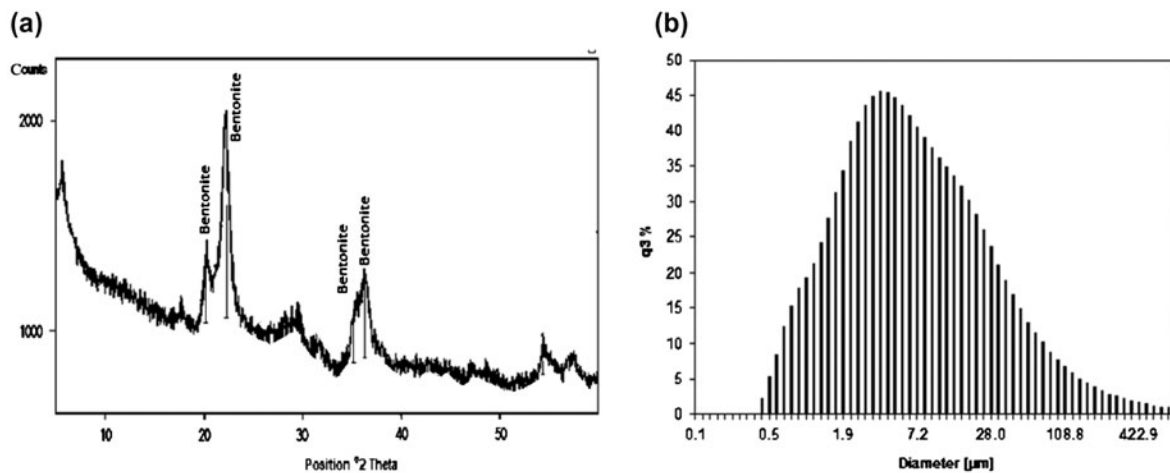


Fig. 2. (a) XRD spectrum and (b) particle size distribution of montmorillonite used in experiments.

3.1. Potentiometric titration results

Fig. 3 shows that even after half of the total base volume is exhausted, the pH of system does not significantly change. This pH region which is resistant to pH change shows a strong buffer effect of adsorbent resulting from deprotonation of permanently negatively charged surface of 1:1 or 2:1 clays [20,21]. In spite of adding more base, steep surge was not observed through alkalimetric titration. It means that the clay surface behaves as weak acid. Upon further examination of titration curve, it can be said that pH_o value of montmorillonite is around pH 6. This is in good agreement with Tombacz's expression which characterized the OH groups at edges having $pH_o \sim 6.5$ as less basic than the Al-OH and less acidic than the Si-OH groups [22]. So, at lower pHs than

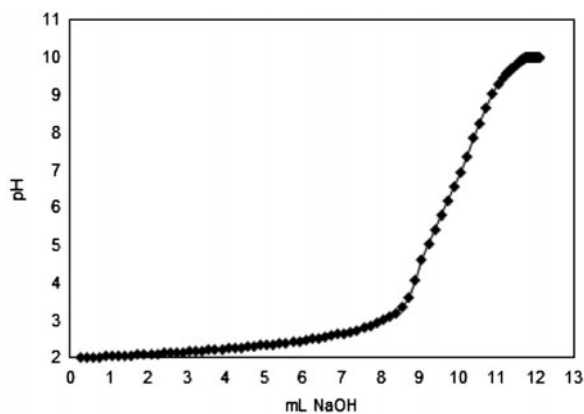


Fig. 3. Potentiometric titration curve for montmorillonite (concentration of clay suspension = 10 g/L, titration rate = 2 mL/min, inert electrolyte concentration = 0.01 M).

pH ~ 6.5 , while silica sites have deprotonated, alumina sites maintain its protonated form. At higher pH values, both silica and alumina sites are negatively charged.

3.2. Kinetics of adsorption

The variation of equilibrium concentration of yellow dye with shaking time is shown in Fig. 4(a). As

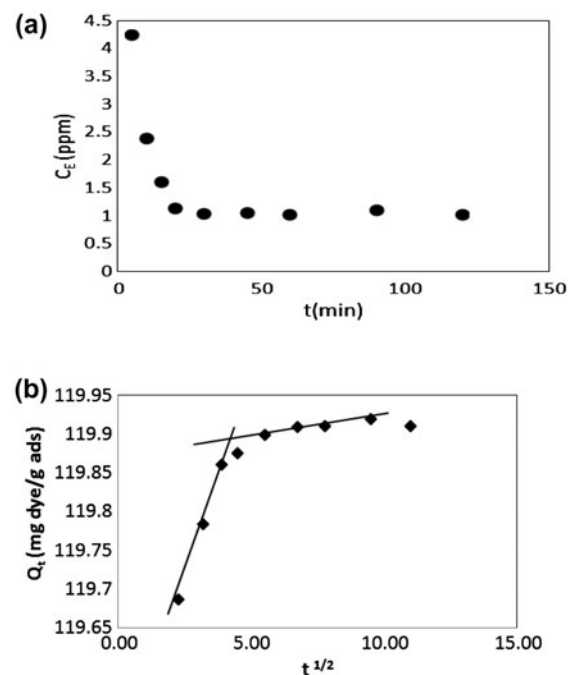


Fig. 4. (a) Effect of contact time on dye adsorption onto montmorillonite, (b) Intraparticle Diffusion for the basic dye adsorption onto montmorillonite ($C_0 = 3,000$ ppm for Yellow 28, solid/liquid ratio = 25 g/L).

observed from Fig. 4(a), 30 min is sufficient for achieving equilibrium. Kinetic of basic dye adsorption was investigated by the aid pseudo-first order and second order model, intraparticle diffusion model and Bangham's model (Eqs. (1)–(4)).

$$\text{Log } (Q_E - Q_t) = \text{Log } Q_E - (k_1/2.303)t \quad (1)$$

where k_1 is the first order rate constant, t is the contact time (min), Q_E is the adsorbed amount of dye at equilibrium, and Q_t is the adsorbed amount of dye at time t . The rate constant (k_1) can be calculated from the slope of the plot between $\text{Log } (Q_E - Q_t)$ and t (Lagergren model) [23,24].

A pseudo-second order model is also used to explain the sorption kinetics. This model is expressed with the equations (Ho and McKay model) [3,23,24]:

$$t/Q_t = 1/k_2 Q_E^2 + (1/Q_E)t \quad (2)$$

where k_2 is II order rate constant and Q_E and Q_t are defined as in the pseudo-first order model.

The mass transfer of adsorbate in adsorption process takes place through several steps:

- (1) Bulk diffusion: when a solid is put into a liquid, electrical double layer occurs beyond solid–liquid interface. The triple-layer model is used for explaining the clay–water interface. Because there is an adsorbate concentration gradient between bulk solution and Outer Helmholtz Plane (OHP), adsorbate ions or molecules migrate from bulk solution to adsorbent surface. This migration is the faster step of adsorption process.
- (2) Film diffusion (boundary layer diffusion): the adsorbate molecules, achieved OHP, are transferred to Inner Helmholtz Plane where the adsorbate ions or molecules are specifically adsorbed (inner-sphere complexation). These two stages are defined as exterior surface adsorption [5].
- (3) Pore diffusion or intraparticle diffusion: when the adsorption of the exterior surface reaches saturation, adsorbate ions or molecules diffuse from the surface to interior of the particle and encounter fresh adsorption sites.

Pseudo-first order and second order models define the bulk diffusion rate. In order to explain the boundary layer and pore diffusion rate, intraparticle

diffusion model is used and expressed as below [3,23,24]:

$$Q_t = k_i t^{1/2} + C \quad (3)$$

where k_i is the intraparticle diffusion rate constant and C is the intercept. As seen from Fig. 4(b), $t^{1/2}$ vs. Q_t curve represents two linear region having different slope and intercept. The first straight line points out boundary layer diffusion and the second line shows intraparticle diffusion with a much lower slope. Consequently, the rate controlling step of the whole adsorption process is the intraparticle diffusion step. This result is in good agreement with the literature [25,26]. Kinetic data were also applied, Bangham's model using Eq. (4);

$$\text{Log } [C_0/(C_0 - Q_t m)] = \text{Log } [(k_0 m)/(2.303 V)] + \alpha \text{Log } t \quad (4)$$

where C_0 is the initial concentration of organic dye (mol L^{-1}), V is the volume of solution (mL), m is solid/liquid ratio (g/L), and k_0 and α are constant [3].

Besides R^2 value, sum of error square percent (SSE %) values of kinetic results were calculated by the aid of Eq. (5) [27]:

$$\text{SSE } \% = \sqrt{\left(\sum (Q_{E,\text{exp}} - Q_{E,\text{cal}})^2\right)/N} \quad (5)$$

where $Q_{E,\text{exp}}$ is the experimental adsorption capacity at equilibrium, $Q_{E,\text{cal}}$ is the calculated adsorption capacity from kinetic models, and N is the number of data points.

The results are shown in Table 1. Basic dye adsorption showed pseudo-second order kinetics, as it is apparent from much higher correlation coefficient (R^2) and lower SSE% value. This result is in good agreement with the literature [28,29].

3.3. Result of isotherm experiments

Fig. 5 shows adsorbed amount of yellow organic dye on montmorillonite samples having different suspension concentration. As seen from the graph, 25 g/L of clay suspension is sufficient for dye adsorption. So, this concentration was used in the adsorption experiments. Experimental data were analyzed using Langmuir, Freundlich, Temkin, and Dubinin–Radushkevich isotherm models and calculated parameters were given in Table 2. Linearized equations are shown below:

Table 1

Kinetic parameters for the Basic Yellow Dye adsorption on montmorillonite (25°C, initial dye conc: 3,000 ppm, and suspension conc: 25 g/L)

	k_1 1/min	k_2 g/mg min	$Q_{E\text{ cal.}}$ (mg/g)	$Q_{E\text{ exp.}}$ (mg/g)	k_i (mg/g min ^{1/2})	C (mg/g)	k_0 L/(mg/L)	α	R^2	SSE%
Pseudo-first order kinetics	0.157		0.471	119.90					0.980	119.35
Pseudo-second order kinetics		0.914	125.00						1.000	5.18
Intraparticle diffusion model					0.088	119.50			0.962	
Bangham's model							241.204	0.662	0.981	

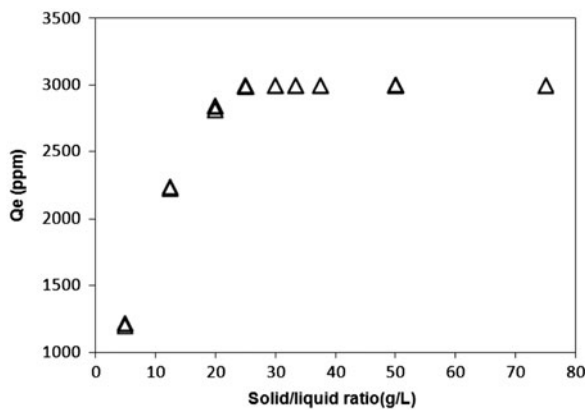


Fig. 5. Basic Yellow 28 adsorption onto montmorillonite as a function of solid/liquid ratio ($C_0 = 3,000$ ppm, $t = 30$ min).

$$C_E/Q_E = 1/(K_1 Q_{max}) + (1/Q_{max})C_E \quad (6)$$

(linearized Langmuir model)

where C_E is the equilibrium concentration of the metal ions (mg/L), Q_E is the specific amount of metal ions

adsorbed (mg/g), Q_{max} is the maximum adsorption capacity (mg/g), and K_1 is the equilibrium constant (L/mg).

$$\text{Log } Q_E = \text{Log } K_F + 1/n \text{ Log } C_E \quad (7)$$

(linearized Freundlich model)

where K_F and n are the Freundlich constants.

$$Q_E = B \text{ Ln } A_T + B \text{ Ln } C_E \quad (8)$$

(linearized Temkin model)

$$B = R \cdot T/b \quad (9)$$

where A_T is the equilibrium constant of binding (L/g), B is the Temkin constant which is related to heat of sorption (J/mol), R is the gas constant (8.314 J/mol K), T is the temperature (K) and b is the Temkin isotherm constant (unitless).

$$\text{Ln } Q_E = \text{Ln } Q_{max} - B_D [RT \text{ Ln } ((C_E + 1)/C_E)]^2 \quad (10)$$

(linearized Dubinin–Redushkevich model)

$$E = 1/(2B_D)^{1/2} \quad (11)$$

Table 2

Isotherm model parameters for both individual and competitive adsorption of basic organic dyes

		Langmuir			Freundlich			Temkin			Dubinin–Radushkevich			
		Q_{max}^a	K	R^2	K_F	n	R^2	B^b	K_t	R^2	B_D	Q_{max}^a	E_D^b	R^2
Yellow 28	Ind.	0.288	2.5	0.99	94.1	8.71	0.92	26.24	1.66	0.94	0.44	0.256	1.93	0.89
	Comp.	0.078	1.7×10^{-2}	0.99	5.41	3.92	0.96	4.01	1.74	0.96	1.20	0.051	0.65	0.73
Red 46	Ind.	2.755	1.2×10^{-3}	0.98	151.32	4.95	0.95	96.81	3.44	0.74	0.14	1.666	1.87	0.52
	Comp.	0.729	3.5×10^{-3}	0.99	50.44	5.30	0.98	25.76	3.32	0.91	0.21	0.451	1.53	0.53
Blue 41	Ind.	3.454	8.9×10^{-4}	0.98	743.87	14.6	0.55	94.67	312.62	0.55	1.9×10^3	2.836	7.87	0.19
	Comp.	0.829	3.6×10^{-3}	0.99	50.44	7.67	0.92	28.19	41.64	0.94	0.29	0.665	1.31	0.83

^aThese values are given as mmol dye/g adsorbent.

^bThese values are given as J/mol.

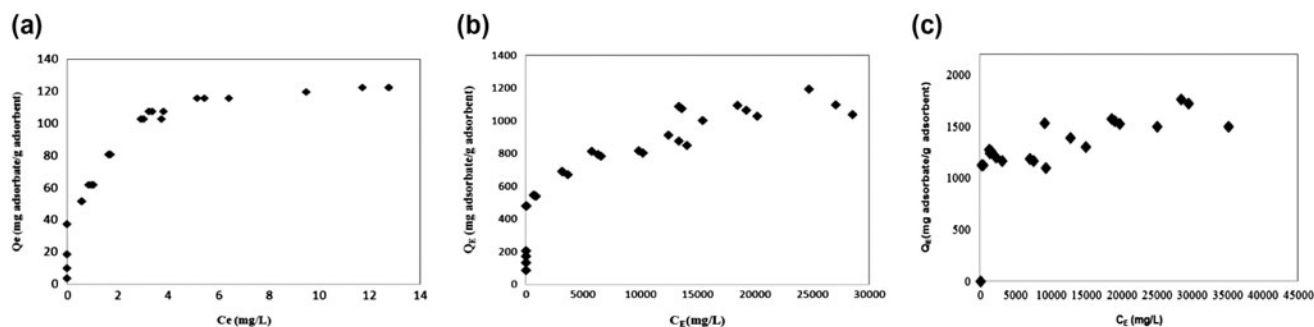


Fig. 6. Organic dye (a) Basic Yellow 28, (b) Red 46, and (c) Blue 41 adsorption as a function of initial concentration of dye working solution (pH 4.5, solid/liquid ratio = 25 g/L, $t = 30$ min).

where Q_s is the theoretical saturation capacity (mg/g), B_D is the constant which is related to the mean free energy of adsorption (mol^2/J^2), and E is the mean free energy of adsorption per mol of adsorbate (J/mol).

Considering Fig. 6(a)–(c) and comparing correlation coefficients (R^2), it is understood that the Langmuir isotherm model fits well with both individual and competitive adsorption experimental data. Similar results are observed from many studies in which cationic dye adsorption on montmorillonite and lignite have been performed [29,30]. Maximum adsorption capacity values are calculated using linearized Langmuir equation. The results tabulated in Table 2 show that Blue 41 has the highest adsorption capacity. Having similar chemical structure, Blue 41 is followed by Red 46. The lowest adsorption capacity is gained for yellow dye adsorption on montmorillonite because of structural difference of Yellow 28 from other dyes used in experiments. The adsorption of cationic organic dyes occurs via electrostatic interaction between positive charges on nitrogen atoms of five-membered cyclic rings and permanently negative charge on silica sites of montmorillonite. Sterical prevention of adjacent aromatic groups in Basic Yellow 28 decreases the dye-surface interaction and causes the lowest adsorption capacity. Dye mixture adsorption onto montmorillonite data are shown in Fig. 7. Comparing the individual adsorption of each dye, competition between dyes does not change Langmuirian character of adsorption. Maximum adsorption capacities of dyes calculated from linearized Langmuir equation significantly decrease because of competition (Table 2). But $Q_{\max \text{ blue}} > Q_{\max \text{ red}} > Q_{\max \text{ yellow}}$ order kept constant in competitive adsorption. SEM-EDS images and graphs of individually blue and yellow dye loaded adsorbents are shown in Fig. 8(a) and (b). EDS-Elemental analysis results proved C and N atoms in loaded adsorbent which comes from organic dye structure. Fig. 9(a) and (b) show cationic organic dye

adsorption on montmorillonite is independent from suspension pH. That the cationic dye adsorption is not affected from deprotonation of surface with increasing pH supports the thought of adsorption taking place on the permanently negatively charged surface of montmorillonite. This result proves that the cationic dye adsorption occurs on permanently negatively charged surfaces (X^-) of montmorillonite. Because of the large structure of the dye, it is sterically prevented

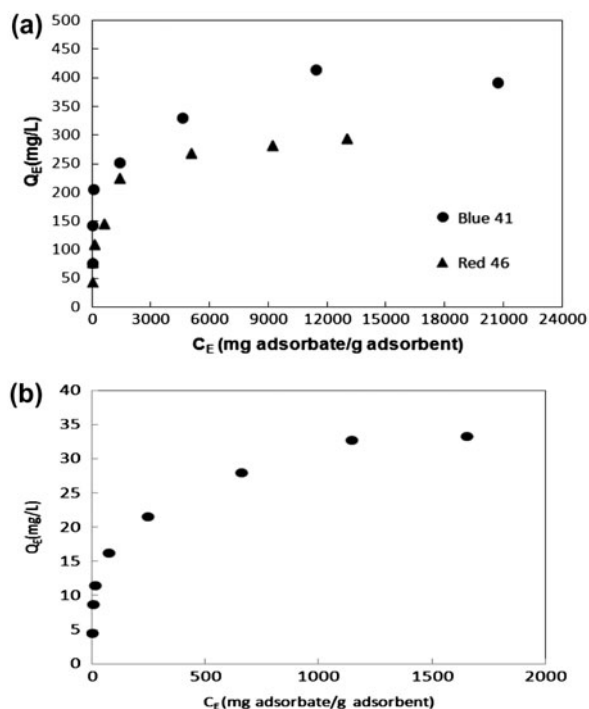


Fig. 7. Isotherm curves of competitive organic dyes ((a) Red 46 and Blue 41 (b) Basic Yellow 28) adsorption onto montmorillonite (pH 4.5, solid/liquid ratio = 25 g/L, $t = 30$ min).

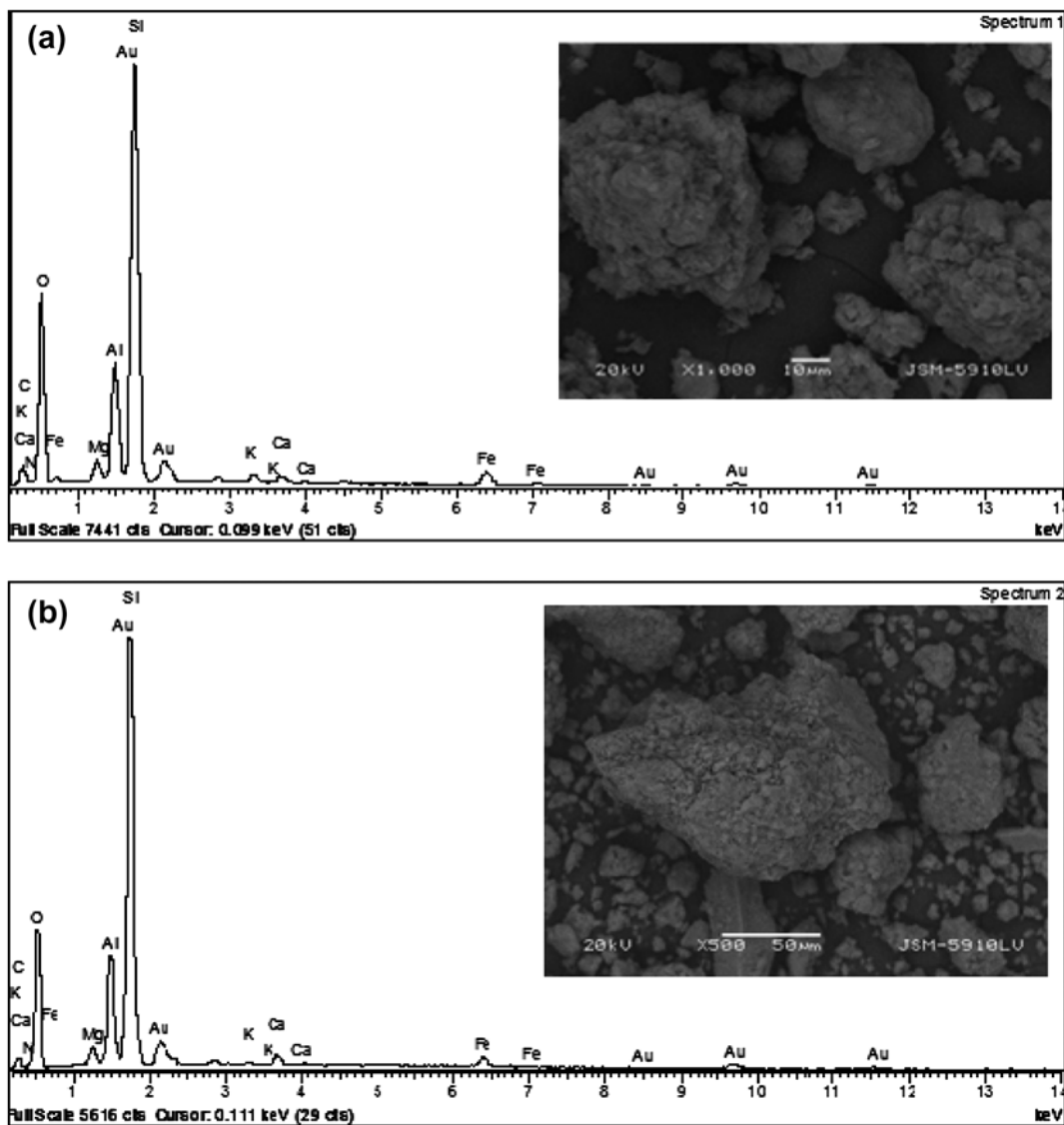


Fig. 8. SEM images and EDS graphs for (a) Basic Yellow 28 and (b) Blue 41 loaded montmorillonite.

from reaching the edge site of the adsorbent where pH-dependent adsorption occurs.

3.4. Result of desorption experiments

Results of leach experiments into sodium humate, CaCl_2 , and acid mixture solutions showed that the retained organic dye onto adsorbent surface does not significantly desorb (Fig. 10). The results obtained from the leaching tests are given in Table 3. Basic organic dye immobilization is higher into 1% sodium humate solution, followed by 0.1 M CaCl_2 solution for Red 46. Red 46 is the most leached organic dye among others. The higher leaching capability of sodium

humate may be due to its hydrophilic and hydrophobic interaction ability (via phenolic $-\text{OH}$ and $-\text{COOH}$ groups or long C chains of humic acid). And it is also observed that the higher sodium humate concentration causes the higher organic dye desorption.

3.5. Results of waste water adsorption

After shaking with 25 g/L montmorillonite for 30 min, COD value of dye-kitchen waste water sample was determined as 240 ppm. The initial COD value of this sample was 10,400 ppm. Turkish "Water Pollution Control Directory" states that the permissible lower discharge COD limits for fiber production textile

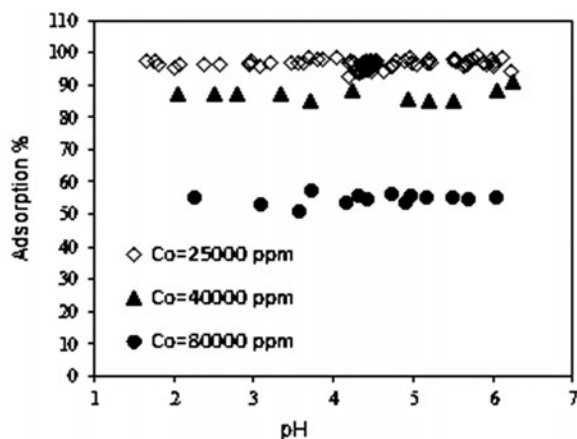


Fig. 9. pH effect on basic organic dye adsorption at different initial Blue 41 concentrations (solid/liquid ratio = 25 g/L, $t = 30$ min) (just one representative graph was given because of similarity between graphs).

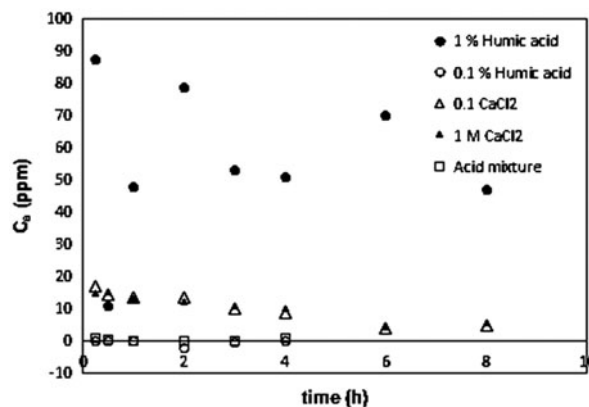


Fig. 10. Leach values of Red 46—loaded montmorillonite into different leachants as a function of leaching time (solid/liquid ratio = 25 g/L, $t = 30$ min) (just one representative graph was given because of similarity between graphs).

Table 3

Organic dyes leach values (in ppm) of dye-loaded montmorillonite for maximum contact time

	Acid mixture (pH 5)	CaCl ₂ solutions		Humic acid solutions	
		0.1 M	1 M	0.1%	1%
Blue 41	Not detected	Not detected	0.06	Not detected	25.02
Red 46	0.84	4.84	5.60	Not detected	46.82
Basic Yellow 28	0.08	2.52	3.68	Not detected	22.15

industrial waste water is 350 and 250 ppm for composite sample picked in 2 h and 24 h, respectively [31]. So, providing the defined conditions in this study, montmorillonite can be used in water treatment process of textile industrial discharges especially for dye-kitchen waste.

4. Conclusion

Montmorillonite surface behaves as a weak acid and has a strong buffer effect in a pH range from 2 to 3.5 resulting from deprotonation of permanently negatively charged surface of montmorillonite. Kinetic parameters indicated that adsorption kinetic fitted II order reaction. The adsorption reactions achieve equilibrium in a short time. The adsorption of cationic organic dyes occurs via electrostatic interaction between positive charges on nitrogen atoms of five-membered cyclic rings and permanently negative charge on silica sites of montmorillonite, which is pH-independent sites and occur as a result of isomorphous substitution. Sterical prevention of adjacent aromatic groups in Basic Yellow 28 decreases the dye-surface

interaction. Lower energy values support the electrostatic interaction between surface and dye molecules. Because basic organic dye adsorption is independent from pH changes, deprotonation of surface with increasing pH does not affect adsorption. In competition, Langmuirian character of adsorption and capacity order did not change, but maximum adsorption capacities of dyes on montmorillonite dramatically decreased. EDS-Elemental analysis results proved that C and N atoms in loaded adsorbent come from organic dye structure.

Retained organic dye on adsorbent surface does not significantly desorb with the exception of desorption into sodium humate solution. Hydrophilic and hydrophobic interaction ability of humic acid via phenolic-OH and -COOH groups or long C chains play an important role in leaching capability of humic acid.

Acknowledgments

The authors thanks to Yalova University Research Fund for their financial support to this study under the

research project 2012/041. Thanks are also extended to AKSA Company (Acrylic Chemical Company) and Re-De Department of Kale Seramik A.Ş. Çanakkale.

References

- [1] K. Shakir, A.F. Elkafrawy, H.F. Ghoneimy, S.G.E. Beheir, M. Refaat, Removal of rhodamine B (a basic dye) and thoron (an acidic dye) from dilute aqueous solutions and wastewater simulants by ion flotation, *Water Res.* 44 (2010) 1449–1461.
- [2] G. Crini, P.M. Badot, Application of chitosan, a natural aminopolysaccharide, for dye removal from aqueous solutions by adsorption processes using batch studies. A review of recent literature, *Prog. Polym. Sci.* 33 (2008) 399–447.
- [3] C.Y. Kuo, C.H. Wu, J.Y. Wu, Adsorption of direct dyes from aqueous solutions by carbon nanotubes: Determination of equilibrium, kinetics and thermodynamics parameters, *J. Colloid Interface Sci.* 327 (2008) 308–315.
- [4] G.Z. Kyzas, N.K. Lazaridis, Reactive and basic dyes removal by sorption onto chitosan derivatives, *J. Colloid Interface Sci.* 331 (2009) 32–39.
- [5] E. Eren, Investigation of a basic dye removal from aqueous solution onto chemically modified Unye bentonite, *J. Hazard. Mater.* 166 (2009) 88–93.
- [6] S.S. Tahir, N. Rauf, Removal of a cationic dye from aqueous solutions by adsorption onto bentonite clay, *Chemosphere* 63 (2006) 1842–1848.
- [7] M. Turabik, Adsorption of basic dyes from single and binary component systems onto bentonite: Simultaneous analysis of Basic Red 46 and Basic Yellow 28 by first order derivative spectrophotometric analysis method, *J. Hazard. Mater.* 158 (2008) 52–64.
- [8] C. Bilgiç, Investigation of the factors affecting organic cation adsorption on some silicate minerals, *J. Colloid Interface Sci.* 281 (2005) 33–38.
- [9] M. Roulia, A.A. Vassiliadis, Sorption characterization of a cationic dye retained by clays and perlite, *Micropor. Mesopor. Mater.* 116 (2008) 732–740.
- [10] B.K. Nandi, A. Goswami, M.K. Purkait, Removal of cationic dyes from aqueous solutions by kaolin: Kinetic and equilibrium studies, *Appl. Clay Sci.* 42 (2009) 583–590.
- [11] A.B. Karim, B. Mounir, M. Hachkar, M. Bakasse, A. Yaacoubi, Removal of Basic Red 46 dye from aqueous solution by adsorption onto Moroccan clay, *J. Hazard. Mater.* 168 (2009) 304–309.
- [12] B.A. Fil, Z. Karakaş, R. Boncukoğlu, A.E. Yılmaz, Removal of cationic dye (Basic Red 18) from aqueous solution using natural Turkish clay, *Global NEST J.* 15 (2013) 529–541.
- [13] B.A. Fil, M.T. Yılmaz, S. Bayar, M.T. Elkoca, Investigation of adsorption of the dyestuff astrazon red violet 3rn (basic violet 16) on montmorillonite clay, *Braz. J. Chem. Eng.* 31 (2014) 171–182.
- [14] E. Aladağ, B.A. Fil, R. Boncukoğlu, O. Sözüdoğru, A.E. Yılmaz, Adsorption of methyl violet dye a textile industry effluent onto montmorillonite-batch study, *J. Dispersion Sci. Technol.* 35 (2014) 1737–1744.
- [15] K. Bessho, C. Degueldre, Generation and sedimentation of colloidal bentonite particles in water, *Appl. Clay Sci.* 43 (2009) 253–259.
- [16] W.K. Mekhamer, Stability changes of Saudi bentonite suspension due to mechanical grinding, *J. Saudi Chem. Soc.* 15 (2011) 361–366.
- [17] M.H. Baik, W.J. Cho, P.S. Hahn, Erosion of bentonite particles at the interface of a compacted bentonite and a fractured granite, *Eng. Geol.* 91 (2007) 229–239.
- [18] M. Zhang, Y. Lu, X. Li, Q. Chen, L. Lu, M. Xing, H. Zou, J. He, Studying the cytotoxicity and oxidative stress induced by two kinds of bentonite particles on human B lymphoblast cells in vitro, *Chem. Biol. Interact.* 183 (2010) 390–396.
- [19] M. Zhang, X. Li, Y. Lu, X. Fang, Q. Chen, M. Xing, J. He, Studying the genotoxic effects induced by two kinds of bentonite particles on human B lymphoblast cells in vitro, *Mutat. Res. Genet. Toxicol. Environ. Mutagen.* 720 (2011) 62–66.
- [20] J. Hizal, R. Apak, Modeling of cadmium(II) adsorption on kaolinite-based clays in the absence and presence of humic acid, *Appl. Clay Sci.* 32 (2006) 232–244.
- [21] J. Hizal, R. Apak, Modeling of copper(II) and lead(II) adsorption on kaolinite-based clay minerals individually and in the presence of humic acid, *J. Colloid Interface Sci.* 295 (2006) 1–13.
- [22] E. Tombácz, M. Szekeres, Colloidal behavior of aqueous montmorillonite suspensions: The specific role of pH in the presence of indifferent electrolytes, *Appl. Clay Sci.* 27 (2004) 75–94.
- [23] P. Sivakumar, N. Palanisamy, Mechanistic study of dye adsorption onto a novel non-conventional low-cost adsorbent, *Adv. Appl. Sci. Res.* 1 (2010) 58–65.
- [24] M. Gouamid, M.R. Ouahrani, M.B. Bensaci, Adsorption equilibrium, kinetics and thermodynamics of methylene blue from aqueous solutions using date palm leaves, *Energ. Procedia* 36 (2013) 898–907.
- [25] R. Dhodapkar, N.N. Rao, S.P. Pande, S.N. Kaul, Removal of basic dyes from aqueous medium using a novel polymer: Jalshakti, *Bioresour. Technol.* 97 (2012) 877–885.
- [26] R. Parimalam, V. Raj, P. Sivakumar, Removal of Acid Green 25 from aqueous solution by adsorption, *Electron. J. Chem.* 9 (2012) 1683–1698.
- [27] S.H. Hu, S.C. Hu, Application of magnetically modified sewage sludge ash (SSA) in ionic dye adsorption, *J. Air Waste Manage. Assoc.* 64 (2014) 141–149.
- [28] A.R. Tehrani-Bagha, H. Nikkar, N.M. Mahmoodi, M. Markazi, F.M. Menger, The sorption of cationic dyes onto kaolin: Kinetic, isotherm and thermodynamic studies, *Desalination* 266 (2011) 274–280.
- [29] A. Hassani, F. Vafaei, S. Karaca, A.R. Khataee, Adsorption of a cationic dye from aqueous solution using Turkish lignite: Kinetic, isotherm, thermodynamic studies and neural network modeling, *J. Ind. Eng. Chem.* 20 (2014) 2615–2624.
- [30] B.A. Fil, C. Ozmetin, M. Korkmaz, Cationic dye (methylene blue) removal from aqueous solution by montmorillonite, *Bull. Korean Chem. Soc.* 33 (2012) 3184–3190.
- [31] Ministerial Regulations on Surface Water Quality Management, Published in the Official Newspaper Issue No: 28483 dated November 30, 2012.